ON THE MOLECULAR STRUCTURE OF DICYCLOPENTADIENYLLEAD

A. ALMENNINGEN, A. HAALAND AND TOVE MOTZFELDT

Department of Chemistry, University of Oslo, Blindern, Oslo 3 (Norway)

(Received October 18th, 1965; in revised form April 5th, 1966)

INTRODUCTION

The infrared absorption spectrum of dicyclopentadienyllead, first prepared by Fischer and Grubert[1], is remarkably similar to that of ferrocene, indicating that the compound possesses some kind of a sandwich structure[2,3]. Since the dipole moment is appreciable[4], 1.29 ± 0.04 D in cyclohexane[5], several workers[2,3] have suggested the bent sandwich structure sketched in Fig. 1. The proton nuclear magnetic resonance spectrum, which at room temperature consists of a single sharp line[3], is consistent with this model if the ligand rings are assumed to rotate.

In an attempt to determine the structure more accurately we have undertaken an investigation of gaseous dicyclopentadienyllead by means of electron diffraction.
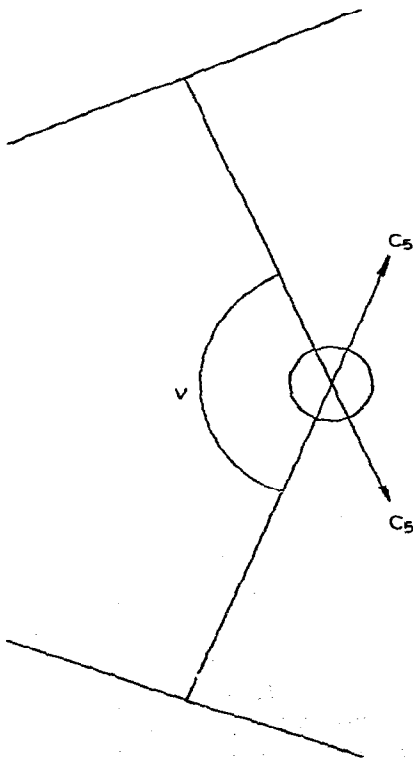

Fig. 1. The molecular structure of $(C_5H_5)_2Pb$.

EXPERIMENTAL AND CALCULATION METHODS*

A sample of $(C_5H_5)_2Pb$ was kindly supplied by Professor E.O. Fischer and used without further purification. The electron diffraction pattern from the gas at $\sim 140°$ was recorded on the Oslo apparatus[8] with two nozzle-to-plate distances, approximately 48 cm and 19 cm, corresponding to s-ranges from 1.5 Å^{-1} to 20 Å^{-1} and from 7 Å^{-1} to 45 Å^{-1}, respectively. $s = 4\pi \sin \theta/\lambda$, where θ is half the scattering angle and λ the electron wavelength. In addition the pattern from $s = 1.25 \text{ Å}^{-1}$ to 5.5 Å^{-1} was recorded on a new similar unit constructed by one of us (A.A.), which permits pictures to be taken with nozzle-to-plate distances up to 180 cm. Four apparently perfect plates covering this low s range, two plates covering the intermediate, and three plates covering the high s range were selected for photometering, and the traces were read off at $\Delta s = 0.25 \text{ Å}^{-1}$ intervals. The plate optical densities were then converted into scattered beam intensities in the usual way. The intensities were corrected for the screening effect of the rotating sector, and empirical "backgrounds" (the part of the total intensity which does not contain information on the molecular structure) were subtracted. The three molecular intensity functions, obtained after multiplication with the modification function $s \cdot |f_C(s)|^{-2}$, were scaled [$f_C(s)$ is the complex atomic scattering factor of carbon, see next paragraph]. The resulting molecular intensity points from $s = 1.25 \text{ Å}^{-1}$ to $s = 35 \text{ Å}^{-1}$ are shown in Fig. 2. Beyond 35 Å^{-1} the pattern was lost in noise.
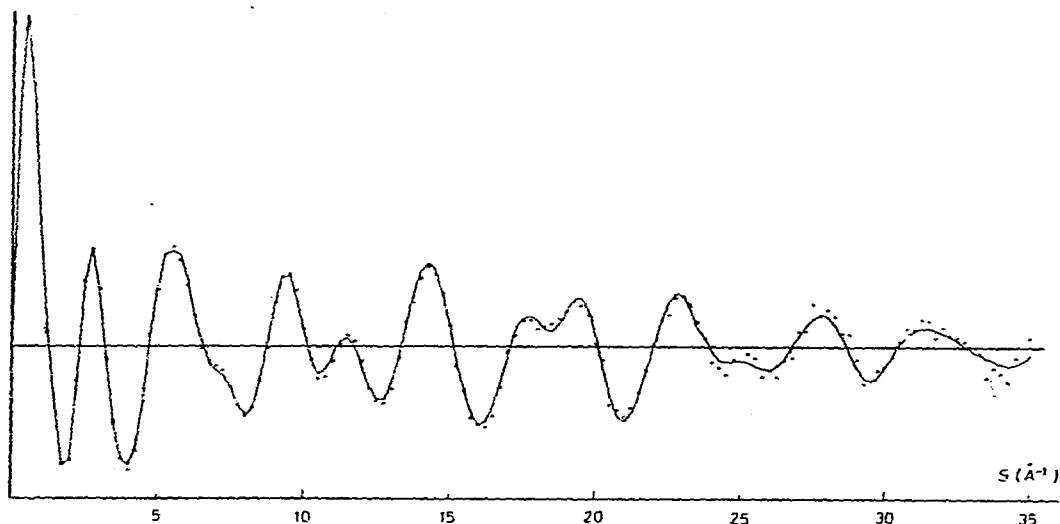

Fig. 2. Theoretical modified molecular intensity curve computed from the parameter values of Table 1 with experimental values drawn in.

The complex atomic scattering factors $f(s) = |f(s)|\exp[i\eta(s)]$ of lead, carbon and hydrogen were computed under the partial wave approximation method outlined by Peacher[9] with a program written by the same author. For hydrogen the exact scattering potential was employed, for carbon the best Hartree–Fock potential[10], and for lead the best Thomas–Fermi–Dirac potential available[11].

---

* For a more thorough discussion of the electron diffraction method see ref. 6 and 7.

Theoretical intensity curves were calculated from

$$I(s) = \Sigma \, \alpha_{ij} \, \frac{|f_i(s)| \, |f_j(s)|}{|f_C(s)|^2} \cos \, [\eta_i(s) - \eta_j(s)] \, \frac{\sin(R_{ij}s)}{R_{ij}} \exp(-\tfrac{1}{2}u_{ij}^2 s^2)$$

$$= \Sigma \, \alpha_{ij} \, g_{ij/CC}(s) \frac{\sin(R_{ij}s)}{R_{ij}} \exp(-\tfrac{1}{2}u_{ij}^2 s^2) \tag{1}$$

The sum extends over all interatomic distances R_{ij} in the molecule. u_{ij} is the root mean square variation of the distance (the vibrational amplitude), $\exp(-\tfrac{1}{2}u_{ij}^2 s^2)$ is often called the "thermal damping" factor. α_{ij} is a constant which should be unity but may be adjusted to compensate for errors in the magnitude—but not the shape— of the $g(s)$ functions, that is in the atomic scattering factors used.

Some structure parameters were refined by a least-squares calculation on the intensity data, i.e. the parameters were selected to minimize the square-error sum

$$\Sigma \, W(s)[I_{obs}(s) - (\text{scalefactor}) \times I_{theor}(s)]^2$$

The weight function, $W(s)$, was unity from $s = 10 \, \text{Å}^{-1}$ to $s = 20 \, \text{Å}^{-1}$, and decreased smoothly to about 0.3 at $1.25 \, \text{Å}^{-1}$ and $35 \, \text{Å}^{-1}$.

Fourier inversion from $s = $ zero to infinity of the theoretical molecular intensity yields a radial distribution (RD) curve like the one shown in Fig. 3. In the RD curve each interatomic distance R_{ij} in the molecule is represented by a peak centered at $r = R_{ij}$. The shape and height of the peak are determined by the vibrational amplitude u_{ij} and by the nature of the $g_{ij/CC}(s)$ function. If the atomic numbers Z_i, Z_j, and Z_C are not too different from each other ($|Z_i - Z_j| < 10, |Z_i - Z_C| < 10$), $g(s)$ is approximately constant and proportional to $Z_i Z_j$. The halfwidth of the peak in the RD curve is then determined by u_{ij} alone, and the area under it is proportional to n_{ij} $Z_i Z_j / R_{ij}$ where n_{ij} is the number of times the distance occurs in the molecule. In the present study all CC, all CH, and all HH distances would be represented by such peaks. But when the three atomic numbers are sufficiently different, as for PbC and PbH distances, the $g_{ij/CC}(s)$ function is no longer a constant, and the picture is more complicated. The peak is then broader than expected from u_{ij} alone, and an "effective atomic number", $Z'_{Pb} \sim 30$, has to be introduced to retain the proportionality of the area with $n_{ij} Z_i Z_j / R_{ij}$.

Since the molecular intensity is observed only from $s = 1.25 \, \text{Å}^{-1}$ to $35.00 \, \text{Å}^{-1}$, the experimental RD curves obtained by Fourier inversion will lack the contributions of the Fourier integral from 0 to $1.25 \, \text{Å}^{-1}$ and from $35.00 \, \text{Å}^{-1}$ to infinity. The latter defect can be remedied by multiplying the observed intensity curve with $\exp(-ks^2)$ before Fourier inversion ($k \sim 0.001 \, \text{Å}^2$). The amplitude of the intensity curve in the high s region then becomes so low that the contribution to the Fourier integral becomes negligible. Comparison with eqn. (1) shows that multiplication with $\exp(-ks^2)$ corresponds to an increase in all vibrational amplitudes, u_{ij}, this factor is therefore commonly referred to as the "artificial damping". The lack of the contribution to the Fourier integral in the low s region on the other hand results in an RD curve which is too low—some times even negative—over the entire range from 0 to 7 Å. This is usually remedied by drawing a smooth zero-line through the points where the RD curve is expected to be zero. In the present case the RD curve does not once fall to zero between 2 Å and 6.5 Å, and the drawing in becomes very haphazard. Since an

erroneous zero-line would lead to an erroneous distribution of area under the curve, it would in turn lead to an erroneous assessment of the number of inter-ligand C. . .C distances in each distance interval and an appreciable error in the angle between the ring planes. An alternate procedure is to include theoretical values for the molecular intensity from $s=0\,\text{Å}^{-1}$ to $1.25\,\text{Å}^{-1}$ computed from a start model before Fourier inversion. The zero-line is then unambigiously fixed. Since the RD curve was relatively insensitive to the choice of start model, the second alternative was adopted for this study.

Theoretical RD curves were computed by Fourier inversion from $s=0\,\text{Å}^{-1}$ to $s=35.00\,\text{Å}^{-1}$ of theoretical intensity curves computed according to eqn. (1).

STRUCTURE ANALYSIS

The $(C_5H_5)_2Pb$ molceule may be regarded as consisting of two pyramidal $(C_5H_5)Pb$ fragments sharing a common apex. The molecular structure is then determined by the structure of each fragment and by the way the fragments are joined, i.e. by the relative orientation of the rings (e.g. whether they are staggered or eclipsed) and by the angle V between the pyramidal axes.
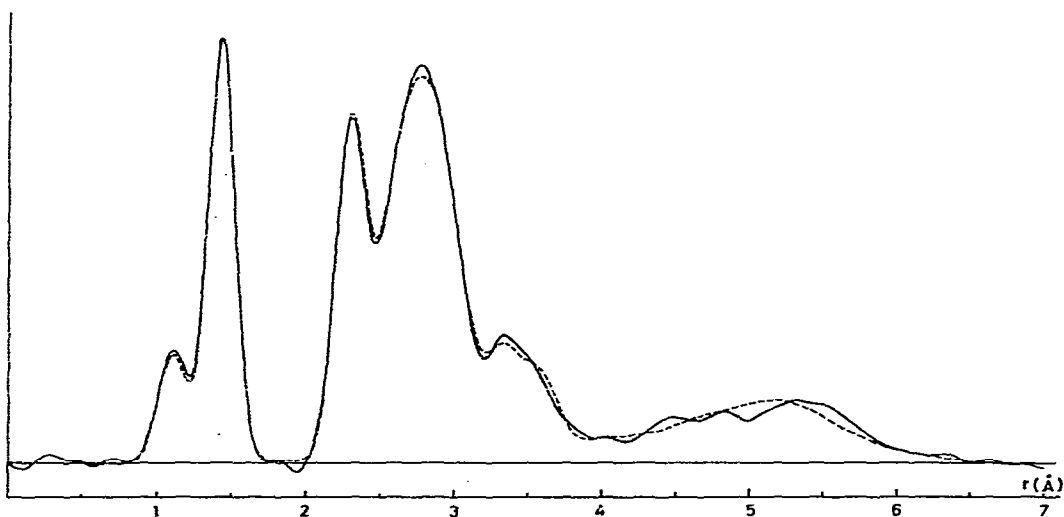

Fig. 3. Radial distribution curves of $(C_5H_5)_2Pb$. —— experimental, --- theoretical computed from the parameter values of Table 1. $k=0.003\,\text{Å}^2$.

An experimental radial distribution (RD) curve is shown in Fig. 3. The assignment of the main peaks is straightforward: The peaks at $1.11\,\text{Å}$ and at $1.43\,\text{Å}$ must correspond to the C–H and C–C bond distances. The peak at $2.3\,\text{Å}$ must be composite, containing peaks corresponding to the C_1. . .H_2 and C_1. . .C_3 nonbonded distances. The broad peak at $2.77\,\text{Å}$ must be assigned to the Pb–C distance (or distances), and the peak at $3.4\,\text{Å}$ to the C_1. . .H_3 and Pb. . .H distances. All intra-ligand and lead–ligand distances are then accounted for, and the complex of unresolved peaks extending out to $6.5\,\text{Å}$ must be due to distances between atoms in different rings. It is at once clear that the ligands cannot be parallel; the shortest inter-ring distance would then

be 5.0 Å. Indeed, it is found that the angle between the pyramidal axes $V \sim 135°$.

The structural parameters of the $Pb(C_5H_5)$ fragments were refined by least-squares calculations on the intensity data under the assumption that both fragments have C_{5v} symmetry and are of equal size. The independent parameters are then the C–C, C–H, and Pb–C bond lengths, the Pb. . .H distance and all interatomic amplitudes. The C_1. . .C_3 and C_1. . .H_2 distances are strongly coupled to the Pb–C distance, and could be greatly influenced by errors in the Pb scattering factors. The C_1. . .H_3 and to some extent the Pb. . .H distances are coupled to the inter-ring distances, that is to the angle V. The C_1. . .C_3, C_1. . .H_2, and C_1. . .H_3 distances were therefore not included in the refinement, but calculated from the C_1–C_2 and C_1–H_1 bond lengths after each cycle. The final refinement was carried out on the staggered $V = 135°$ model described below, and the resulting parameters are listed in Table 1. The error limits of the amplitudes are 3 × the standard deviations obtained. Hence they do not include the effect of possible systematic errors. These are difficult to assess, but experience suggests that their inclusion would increase the error limits by a factor between 1.5 and 3.0. The error limits of the interatomic distances (3 × standard deviations) do include our estimate of possible systematic errors.

The C–C bond length and amplitude are very similar to the corresponding parameters in ferrocene[12] (1.429 Å ± 0.005 Å and 0.046 Å ± 0.005 Å), supporting our assumption that the ligands have C_{5v} symmetry.

The "fudge-factor" α_{Pb-C} [see eqn. (1)] was refined along with the bond length and amplitude. The resulting value was $\alpha = 1.02 \pm 0.08$, which indicates that the magnitude of the $g_{PbC/CC}(s)$ function is about right. The rather large uncertainty may, however, indicate that the shape is not altogether perfect. R_{Pb-C} and u_{Pb-C} did not change significantly when α_{Pb-C} was included in the refinement. The M–C bond length and amplitude correspond to what one might expect in an "ionic" sandwich molecule: In $(C_5H_5)_2Mn$ M–C = 2.382 Å ± 0.011 Å[11]. The ionic radius of Pb^{2+} is 0.41 Å greater than that of Mn^{2+}. The Mn–C amplitude is 0.127 Å ± 0.006 Å[13], which is comparable to the Pb–C amplitude. Both are significantly greater than the M–C amplitude in ferrocene ($u = 0.062$ Å ± 0.003 Å) reflecting the weaker bonding in these compounds.

The large standard deviation of the Pb. . .H distance and the large standard deviations and unreasonably low value for Pb. . .H and C_1. . .H_3 amplitudes reflect the coupling of these parameters to the poorly determined inter-ring parameters. The Pb. . .H distance is not significantly different from that expected if the ligands are planar (3.410 Å).

Fig. 3 shows a theoretical RD curve computed from the parameter values listed in Table 1 (and the staggered $V = 135°$ model described below). The agreement with the experimental curve is good out to 3.5 Å. The slight difference between the Pb–C peaks around 2.8 Å is probably due to errors in the $g(s)$ function. But since it might indicate that our assumption that the $(C_5H_5)Pb$ fragments have C_{5v} symmetry is unwarrented, refinements were carried out on another, less symmetric, model: the lead atom was assumed to be placed equally far above each ligand, equally far from the fivefold symmetry axis of each. The Pb–C distances are then no longer equal. The refinement converged giving a model in which the lead atom was moved 0.26 Å ± 0.06 Å away from the fivefold axes. But the error sum decreased with less than one per cent, and RD curves computed from this model was no great improvement over

previous ones. A certain improvement in the fit is always to be expected on the inclusion of another adjustable parameter. Moreover, a small error in the shape of the $g_{PbC/CC}(s)$ function, e.g. in the zero-point of the cosine factor would be partly compensated for by the introduction of an apparent inequality of the Pb–C distances. (When other—and we believe less accurate—scattering factors were employed, the fit was vastly improved when the possibility of asymmetry was considered). We therefore do not consider this result significant evidence for deviation from C_{5v} symmetry of the $(C_5H_5)Pb$ fragments, though such an asymmetry cannot be ruled out.

TABLE 1

THE MOLECULAR PARAMETERS OF $(C_5H_5)_2Pb$

	$r_g(1)$ $(Å)^a$	u $(Å)^b$
$C_1–C_2$	1.430 ± 0.007	0.045 ± 0.005
$C_1 \ldots C_3$	$(2.314)^c$	0.060 ± 0.008
$C_1–H_1$	1.105 ± 0.018	0.049 ± 0.016
$C_1 \ldots H_2$	$(2.264)^c$	0.048 ± 0.018
$C_1 \ldots H_3$	$(3.383)^c$	0.063 ± 0.045
Pb–C	2.778 ± 0.016	0.142 ± 0.013
Pb $\ldots$ H	3.421 ± 0.040	0.090 ± 0.023
C $\ldots$ C'		0.250
$V=$	$135° \pm 15°$	

^{a} The error limits (3 × standard deviations) include our estimate of possible systematic errors. ^{b} The error limits do not include possible systematic errors. ^{c} Calculated from $C_1–C_2$ and $C_1–H_1$.

When the parameters determining the way the $(C_5H_5)Pb$ fragments are joined were refined by least-squares calculations, the resulting structure was too dependent on the weighting of the data below $s = 10 Å^{-1}$ and the background in the same region to be meaningful. Instead a search for the best model was carried out by comparison of experimental and theoretical RD-curves in the region 3.5 Å to 6.5 Å. The angle between the pyramidal axes V, the relative orientation of the ligand rings, and the C $\ldots$ C' u-values were varied systematically, and the possibility of large amplitude variation of V was considered, but it proved impossible to find a model that gave perfect agreement. In particular it was impossible to find any model that reproduced the shallow minimum at 5.0 Å. To achieve maxima and minima in the theoretical curve of a height similar to those found in the experimental curve, it was necessary to use inter-ligand C $\ldots$ C amplitudes of 0.15 Å or less. This in itself appears unreasonable; in $(C_5H_5)_2Mn$ the corresponding amplitudes are about 0.25 Å[13]. We therefore conclude that the slight maxima and minima found in the 3.5 Å to 6.5 Å region of the experimental RD curve are spurious.

The theoretical curves were sensitive mainly to the angle V, much less so to the relative orientation of the rings. It was therefore possible to determine V roughly, $V = 135 \pm 15°$ while the relative orientation of the rings remains unknown. They probably undergo free or only slightly hindered rotation.

Fig. 3 shows a theoretical RD curve computed from a staggered C_s molecular model with $V = 135°$, all inter-ring amplitudes $u = 0.25$ Å, and the parameter values listed in Table 1. Fig. 2 shows the theoretical modified molecular intensity curve computed for the same model.

APPENDIX

Since $(C_5H_5)_2Sn$ probably has a structure similar to that of $(C_5H_5)_2Pb$, a study of this compound was initiated. In this case, however, the recording of the diffraction pattern proved difficult: The primary beam would be deflected in the neighbourhood of the nozzle. The reason probably was that the molecules—or fragments—reaching the cold trap surrounding the nozzle were negatively charged, resulting in strong electrostatic fields. Indeed, the deflection could be largely depressed by the suspension of a grating in front of the cold trap. Even then the data were plagued by a background of extraneous scattering, and the pattern was lost in noise beyond $s = 24.0$ Å^{-1}. Though the data were poor, and even though the effect may indicate that disintegration of the sample was taking place, they were processed in the same way as for $(C_5H_5)_2Pb$.

The resulting RD curves were very similar to the ones in Fig. 3, though the noise level was higher. No signs of disintegration were found, it certainly cannot have exceeded 20%. Least-squares refinements on the intensity gave:

	$r_g(1)$ (Å)	u (Å)
C–C	1.431 ± 0.009	0.044 ± 0.019
Sn–C	2.706 ± 0.024	0.156 ± 0.027
C–H	1.142 ± 0.056	0.073 ± 0.059

As before, the error limits are $3 \times$ the standard deviations. From the RD curves it was again clear that the ligand rings could not be parallel, $V \sim 125°$.

ACKNOWLEDGEMENT

SUMMARY

The electron scattering pattern from gaseous $(C_5H_5)_2Pb$ has been recorded from $s = 1.25$ Å^{-1} to 35.0 Å^{-1}. Beyond this point the molecular intensity is lost in the background. The bond lengths are: $C_1-C_2 = 1.430 \pm 0.006$ Å, $C_1-H_1 = 1.105 \pm 0.018$ Å, Pb–C $= 2.778 \pm 0.016$ Å. The ligand rings are not parallel, the angle between the planes being $45° \pm 15°$.

The scattering pattern from $(C_5H_5)_2Sn$ has been recorded from $s = 1.25$ Å^{-1} to 24.0 Å^{-1}. The bond lengths are $C_1-C_2 = 1.431 \pm 0.009$ Å, $C_1-H_1 = 1.142 \pm 0.056$ Å, Sn–C $= 2.706 \pm 0.024$ Å. The ligand rings are not parallel, the angle between the planes being about $55°$.

REFERENCES

1 E. O. FISCHER AND H. GRUBERT, Z. Anorg. Chem., 286 (1956) 237.
2 H. P. FRITZ AND E. O. FISCHER, J. Chem. Soc., (1961) 547.

3 L. D. Dave, D. F. Evans and G. Wilkinson, *J. Chem. Soc.*, (1959) 3684.
4 E. Weiss, *Z. Anorg. Chem.*, 287 (1956) 236.
5 E. O. Fischer and S. Schreiner, *Chem. Ber.*, 92 (1959) 938.
6 G. Bastiansen and P. N. Skancke, *Advan. Chem. Phys.*, 3 (1960) 323.
7 A. Almenningen, O. Bastiansen, A. Haaland and H. M. Seip, *Angew. Chem. Intern. Ed. Engl.*, 4 (1965) 819.
8 O. Bastiansen, O. Hassel and I. Risberg, *Acta Chem. Scand.*, 9 (1955) 232.
9 J. L. Peacher, Ph. D. Thesis, Department of Physics, Indiana University, Bloomington, Indiana, 1965.
10 T. G. Strand and R. A. Bonham, *J. Chem. Phys.*, 40 (1964) 1668.
11 R. A. Bonham and T. G. Strand, *J. Chem. Phys.*, 39 (1963) 2200.
12 R. K. Bohn and A. Haaland, *J. Organometal. Chem.*, 5 (1966) 470.
13 A. Almenningen, A. Haaland and T. Motzfeldt, to be published.